Molecular dynamics study of mesophase formation using a transverse quadrupolar Gay-Berne model

M. P. Neal[1] and A. J. Parker[2]
[1]*School of Mathematical and Information Sciences, Coventry University, Coventry CV1 5FB, United Kingdom*
[2]*School of Mathematics and Computing, University of Derby, Derby DE22 1GB, United Kingdom*
(Received 22 June 2000; published 21 December 2000)

The effect of the transverse electric quadrupole moment on the formation of liquid-crystal mesophases was investigated by means of a computer-simulation study. A simple model of the molecular interaction employed the addition of a transverse, point quadrupole to a Gay-Berne potential. The transverse quadrupole was seen to raise the temperature of onset of the smectic phase. A large magnitude quadrupole stabilized the smectic-*A* phase over the temperature range studied compared to a Gay-Berne reference fluid. The presence of a large quadrupole stabilized cubic smectic phases rather than the more usual hexagonal smectic-*B* phases.

DOI: 10.1103/PhysRevE.63.011706 PACS number(s): 61.30.−v, 61.20.Ja

I. INTRODUCTION

Computer simulation is proving increasingly useful as a technique to relate complex molecular characteristics to experimental measurement and theoretical prediction of material properties. The electrical and optical properties of liquid crystals make them of considerable technological importance [1] in applications such as piezoelectric transducers and nonlinear optics. As such they have been the subjects of an increasing number of simulation and theoretical studies, particularly of polar liquid crystals.

There has been considerable interest in understanding which molecular features of liquid crystals influence the formation of nematic, smectic-*A* and smectic-*C* phases. Theoretical studies are divided as to whether smectic-*C* formation is determined by dipole interactions [2–4], by quadrupole interaction [5,6], by steric interaction [7–9], or by different mechanisms in different systems.

Recent extensive simulation studies of polar liquid crystals have employed a point dipole together with a mesogenic potential, either a hard potential (e.g., [10–12]) or a potential that has attractive and repulsive terms such as the Gay-Berne potential (e.g., [13,14]). The magnitude, direction, whether longitudinal or transverse, and location of the dipole, whether central or terminal, have been shown to have a marked effect on the local molecular correlations in the smectic layers [10–14].

Less attention has been paid to the effect of the electric quadrupole moment on liquid crystal phase behavior. It has been shown to have a significant effect upon the thermodynamic and structural properties of liquid benzene [15] and upon its crystal structure. The molecules in the crystal assemble with edge-to-face pairs as well as pairs in which the molecular disks are parallel but displaced in a face-to-face arrangement [16]. The presence of longitudinal electric quadrupoles in discotic liquid crystals was offered as an explanation to account for many of the features of chemically induced mixtures, including disruption of the columnar phase [17]. There have been several computer studies (e.g., [18,19]) of the phase diagrams of quadrupolar molecules. In one study [18] the quadrupole was found to stabilize solid structures, which are not close-packed monoclinic or plastic crystal but rather orthorhombic or α-N_2, depending on the quadrupole magnitude. This agrees with experimental evidence that nitrogen and oxygen molecules with a small quadrupole moment freeze into a plastic crystal whereas acetylene and carbon dioxide molecules with a large quadrupole moment freeze into an α-N_2 structure. The halogens Cl_2, Br_2, and I_2 with an intermediate quadrupole value, freeze into an orthorhombic structure. In the second simulation study of a soft spherical model with a point dipole the addition of a linear quadrupole [19] was seen to raise the density of the isotropic to nematic and nematic to solid phase transitions, another packing effect.

A recent simulation study by the authors of a system of prolate Gay-Berne particles with longitudinal quadrupoles [20] demonstrated that the formation of the smectic phase is sensitive to the magnitude of the quadrupole. Conditions of a fixed temperature and pressure were employed and nematic, smectic-*A*, smectic-*C* and smectic-*B* phases were observed as the quadrupole was reduced in magnitude. A smectic-*C* phase for a quadrupolar Gay-Berne fluid with different parameters has also been observed [21].

Following on from this, the paper reported here investigates the effect of the addition of a transverse quadrupole upon the phase diagram of a Gay-Berne fluid and solid. This paper in organized as follows. In Sec. II we describe the model. The details of the simulation are discussed in Sec. III and the results are presented in Sec. IV with conclusions in Sec. V.

II. MODEL

The interaction between the molecules was modelled by a biaxial potential comprising an anisotropic Gay-Berne [22] potential together with a transverse point quadrupole [23,24], located at the center of the prolate ellipsoid, and takes the form:

$$U^*(\hat{\mathbf{u}}_i,\hat{\mathbf{u}}_j,\hat{\mathbf{v}}_i,\hat{\mathbf{v}}_j,\hat{\mathbf{r}}_{ij}) = U^*_{\mathrm{GB}}(\hat{\mathbf{u}}_i,\hat{\mathbf{u}}_j,\hat{\mathbf{r}}_{ij}) + U^*_{QQ}(\hat{\mathbf{v}}_i,\hat{\mathbf{v}}_j,\hat{\mathbf{r}}_{ij}), \tag{1}$$

where

$$U^*_{\mathrm{GB}}(\hat{\mathbf{u}}_i,\hat{\mathbf{u}}_j,\hat{\mathbf{r}}_{ij}) = 4\varepsilon(\hat{\mathbf{u}}_i,\hat{\mathbf{u}}_j,\hat{\mathbf{r}}_{ij}) \times\left[\left(\frac{\sigma_0}{r-\sigma(\hat{\mathbf{u}}_i,\hat{\mathbf{u}}_j,\hat{\mathbf{r}}_{ij})+\sigma_0}\right)^{12} -\left(\frac{\sigma_0}{r-\sigma(\hat{\mathbf{u}}_i,\hat{\mathbf{u}}_j,\hat{\mathbf{r}}_{ij})+\sigma_0}\right)^{6}\right] \quad (2)$$

and

$$U^*_{QQ}(\hat{\mathbf{v}}_i,\hat{\mathbf{v}}_j,\hat{\mathbf{r}}_{ij}) = \frac{3Q_i^*Q_j^*}{4r^5}[1+2(\hat{\mathbf{v}}_i\cdot\hat{\mathbf{v}}_j)^2-5(\hat{\mathbf{r}}_{ij}\cdot\hat{\mathbf{v}}_i)^2 -5(\hat{\mathbf{r}}_{ij}\cdot\hat{\mathbf{v}}_j)^2-20(\hat{\mathbf{v}}_i\cdot\hat{\mathbf{v}}_j)(\hat{\mathbf{r}}_{ij}\cdot\hat{\mathbf{v}}_i)(\hat{\mathbf{r}}_{ij}\cdot\hat{\mathbf{v}}_j) +35(\hat{\mathbf{r}}_{ij}\cdot\hat{\mathbf{v}}_i)^2(\hat{\mathbf{r}}_{ij}\cdot\hat{\mathbf{v}}_j)^2]. \quad (3)$$

Here $\mathbf{r}_{ij}$ is the vector linking the centers of mass of the two molecules, $\hat{\mathbf{u}}_i$ and $\hat{\mathbf{u}}_j$ are unit vectors along the molecular axes of symmetry, and $\hat{\mathbf{v}}_i$ and $\hat{\mathbf{v}}_j$ are unit vectors perpendicular to the molecular axes of symmetry. Q_i^* and Q_j^* represent the quadrupole moments of molecules i and j, where Q_i^* $[=Q_i/(4\pi\varepsilon_0\in_0\sigma_0^5)^{1/2}]$ is the dimensionless moment and $\in_0$ is the permittivity of free space. The strength $\varepsilon(\hat{\mathbf{u}}_i,\hat{\mathbf{u}}_j,\hat{\mathbf{r}}_{ij})$ and range $\sigma(\hat{\mathbf{u}}_i,\hat{\mathbf{u}}_j,\hat{\mathbf{r}}_{ij})$ anisotropy functions of the Gay-Berne potential are defined in the Appendix. Following previous studies [25–27] the exponents are assigned the values $\mu=2$, $\upsilon=1$ and the ratio of the end-to-end to side-to-side well depths $\varepsilon_e/\varepsilon_s=0.2$. The shape anisotropy, given by the ratio of separations when $U_{\mathrm{GB}}=0$ for molecules in the end-to-end and side-to-side configurations was assigned the value $\sigma_e/\sigma_s=4$. This includes a region of stability for the smectic-*A* as well as the smectic-*B* phase [27] for a Gay-Berne fluid. Utilizing parameters from a study mapping the Gay-Berne potential on to *p*-terphenyl [28] we set $\sigma_0=3.65\times10^{-10}$ m and $\varepsilon_0/k=4302$ K. The quadrupole moment for benzene has been measured to be -3.0×10^{-39} C m^2 [29]. This leads to an estimate of Q^* of -0.44 for benzene. It is difficult to assess the appropriate value for the quadrupole and in this simulation study a wide range of values of Q^* of -1.0, -0.5 and -0.1 were utilized. Magnitudes of Q^* of 0.1 and 0.05 were used in a recent study of mixtures of quadrupolar Gay-Berne discs [17], overlapping with the range of magnitudes considered here.

Figure 1 shows potential-energy contours for parallel particles interacting via the total potential for values of Q^* of -0.1, -0.5, and -1.0 as a function of their separation and orientation with respect to the intermolecular vector $\mathbf{r}_{ij}$, for fixed $\hat{\mathbf{u}}_i\cdot\hat{\mathbf{u}}_j$, $\hat{\mathbf{v}}_i\cdot\hat{\mathbf{v}}_j$, $\hat{\mathbf{v}}_i\cdot\hat{\mathbf{u}}_i$, and $\hat{\mathbf{v}}_j\cdot\hat{\mathbf{u}}_j$. The shape of the molecules may be defined as the closed contour corresponding to the change in potential energy from positive to negative. Since the quadrupolar contribution depends on the separation between the particles, it has its greatest contribution, whether positive or negative, when the molecules are in the side-to-side configuration. While $\hat{\mathbf{v}}_i\cdot\hat{\mathbf{u}}_i=\hat{\mathbf{v}}_j\cdot\hat{\mathbf{u}}_j=0.0$ for a transverse quadrupole and $\hat{\mathbf{u}}_i\cdot\hat{\mathbf{u}}_j=1.0$ for parallel particles, there are three possible combinations for $\hat{\mathbf{v}}_i$ and $\hat{\mathbf{v}}_j$ in which $\hat{\mathbf{v}}_i\cdot\hat{\mathbf{v}}_j=1.0$ or 0.0: (a) parallel to each other and $\hat{\mathbf{r}}_{ij}\wedge\hat{\mathbf{u}}_j$ with $\hat{\mathbf{v}}_i\cdot\hat{\mathbf{v}}_j=1.0$, (b) parallel to each other and perpendicular to $\hat{\mathbf{r}}_{ij}\wedge\hat{\mathbf{u}}_j$ with $\hat{\mathbf{v}}_i\cdot\hat{\mathbf{v}}_j=1.0$, and (c) one parallel to $\hat{\mathbf{r}}_{ij}\wedge\hat{\mathbf{u}}_j$ and one perpendicular to $\hat{\mathbf{r}}_{ij}\wedge\hat{\mathbf{u}}_j$ with $\hat{\mathbf{v}}_i\cdot\hat{\mathbf{v}}_j=0.0$.

In (a) the quadrupoles remain parallel to one another with varying $\mathbf{r}_{ij}$, whereas in (b) they vary from end-to-end to side-to-side configurations, and in (c) the quadrupoles remain in a '*T*' or cross configuration. The quadrupole potential favors the '*T*' configuration with negative interaction energy. The end-to-end, cross and side-to-side interactions all have positive interaction energy. Figure 1(d) shows a reference Gay-Berne interaction for comparison purposes. Figures 1(c)(i–iii) show the effect of the addition of transverse quadrupoles in the '*T*' configuration for various magnitudes of Q^*. The central energy minimum is deepened with increasing Q^* compared to the Gay-Berne potential without a quadrupole. This is illustrated by the closer spacing of the potential-energy contours in 1(c)i with $Q^*=-1.0$ compared to 1(c)ii with $Q^*=-0.5$; little effect is seen for $Q^*=-0.1$. Figures 1(b)(i–iii) illustrate the effect of the addition of the positive end-to-end and side-to-side interaction of the transverse quadrupoles. The central energy minimum is reduced in all cases and replaced with two energy minima displaced parallel to the major axis of the molecules. For $Q^*=-1.0$ the positive contribution of the quadrupole replaces the central minimum with a small central positive potential indicated by the innermost contour. The effect of the side-to-side and end-to-end contributions of the quadrupoles when perpendicular to $\hat{\mathbf{r}}_{ij}\wedge\hat{\mathbf{u}}_j$ is less marked than when parallel as seen in Figures 1(a)(i–iii). With $Q^*=-1.0$ the central minimum is replaced with two minima displaced parallel to the major axis, however $Q^*=-0.5$ and -0.1 merely reduced the depth of the central minimum. The biaxial nature of the combined potential favors the '*T*' configurations illustrated in Figs. 1(c) with differing effects on the final solid structure, and we will return to this in the discussion of the results.

III. MOLECULAR-DYNAMICS SIMULATIONS

Simulation studies reported here were undertaken in the isothermal-isobaric ensemble (NPT) for systems of $N=500$ particles in a cubic box. Periodic boundary conditions were employed and all simulations were undertaken at a reduced pressure $P^*(=P\sigma_0^3/\varepsilon_0)$ of 2.0. NPT studies to enable structures formed within the box to adjust so that they are commensurate with their periodic boundary images and are not artifacts of the boundary conditions. A reduced pressure of 2.0 was selected since at higher pressure the nematic phase is stable [27]. A reduced time step, $\Delta t^*[=\Delta t(m\sigma_0^3/\varepsilon_0)]$ of 0.0075 was employed together with a cutoff of 5.5 σ_0 and a list radius of 5.8 σ_0. Further details of the molecular-dynamics technique are provided elsewhere [20].

The starting point for the $|Q^*|=1.0$ simulations was an isotropic Gay-Berne fluid with $|Q^*|=0.0$. The magnitude of Q^* was increased to 1.0 at $T^*(=k_BT/\varepsilon_0)$ of 5.5 and the system equilibrated for a sufficient period to determine that it was an isotropic state point. Each starting configuration was taken from the previous temperature and the temperature was lowered in steps of 0.5 until it reached $T^*=1.0$, and then

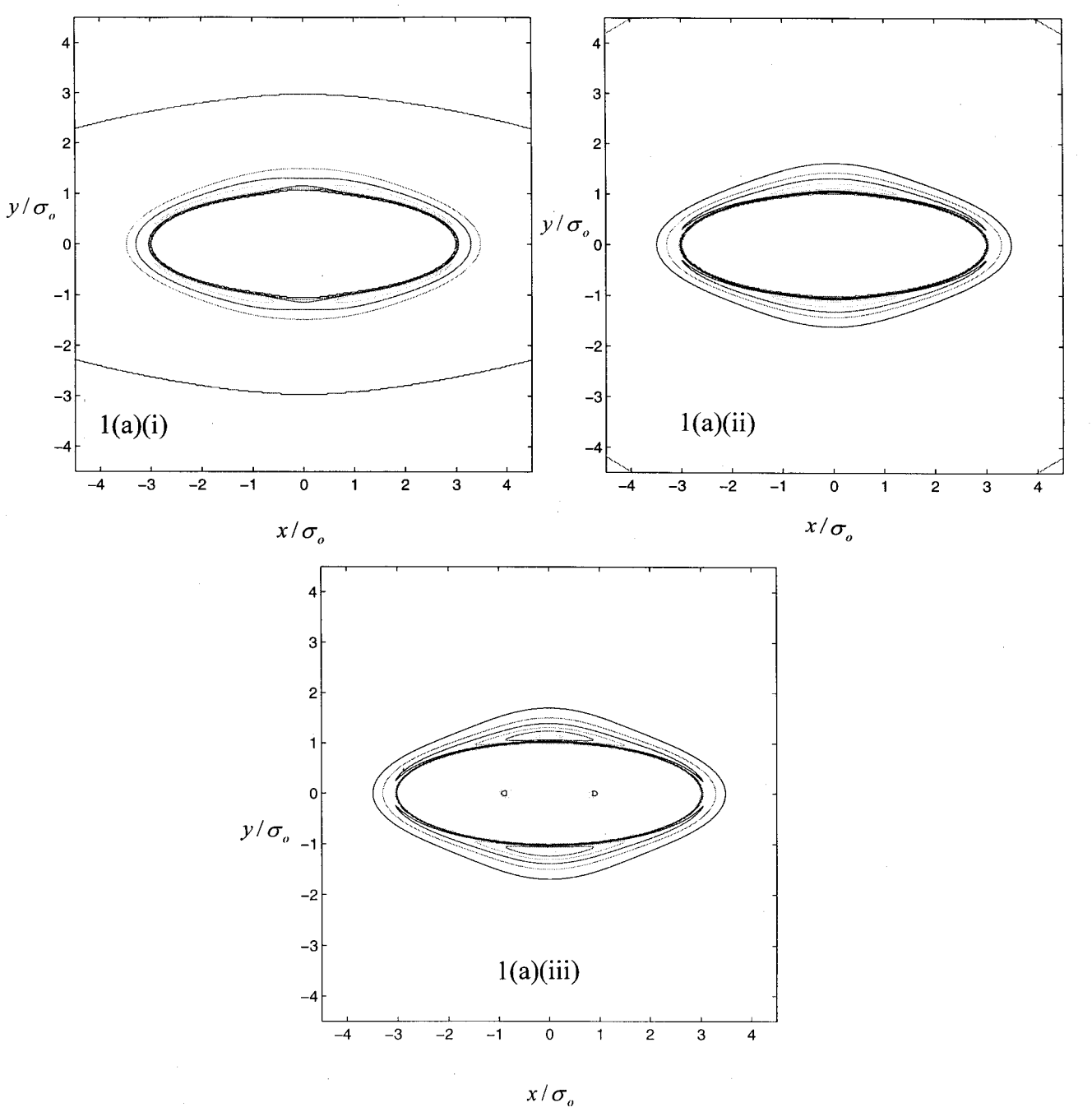

FIG. 1. Potential-energy contours calculated for parallel molecules interacting via the Gay-Berne potential ($\hat{\mathbf{u}}_i \cdot \hat{\mathbf{u}}_j = 1.0$) together with an additional transverse quadrupole for (a) the quadrupoles parallel to each other and $\hat{\mathbf{r}}_{ij} \wedge \hat{\mathbf{u}}_j$ with $\hat{\mathbf{v}}_i \cdot \hat{\mathbf{v}}_j = 1.0$, (b) the quadrupoles parallel to each other and perpendicular to $\hat{\mathbf{r}}_{ij} \wedge \hat{\mathbf{u}}_j$ with $\hat{\mathbf{v}}_i \cdot \hat{\mathbf{v}}_j = 1.0$, and (c) one quadrupole parallel to $\hat{\mathbf{r}}_{ij} \wedge \hat{\mathbf{u}}_j$ and one perpendicular to $\hat{\mathbf{r}}_{ij} \wedge \hat{\mathbf{u}}_j$ with $\hat{\mathbf{v}}_i \cdot \hat{\mathbf{v}}_j = 0.0$; for (i) $Q^* = -1.0$, (ii) $Q^* = -0.5$, and (iii) $Q^* = -0.1$, and for (d) a reference Gay-Berne fluid.

finally lowered to 0.9. Extremely long equilibration runs of up to 1.5×10^6 steps were undertaken where required in the regions where a phase transition was occurring to allow metastable states to equilibrate. A similar procedure was undertaken for the quadrupolar Gay-Berne fluids with $|Q^*|$ of 0.5 and 0.1. Cooling was undertaken through a more limited range of temperatures before a crystal phase was obtained in the latter two cases.

In order to provide a comparison with a system with $|Q^*| = 0.0$, an isotropic configuration at $T^* = 2.0$ obtained from previous work was taken as a starting point and the system cooled to $T^* = 1.0$ in steps of 0.1.

Analysis of the orientational structure was undertaken by use of the second rank order parameters Q_{20}^2 and Q_{22}^2 evaluated using the $\mathbf{Q}$ tensor defined by

$$Q_{\alpha\beta} = \frac{1}{N} \sum_{i=1}^{N} \frac{3u_i^\alpha u_i^\beta - \delta_{\alpha\beta}}{2}, \tag{4}$$

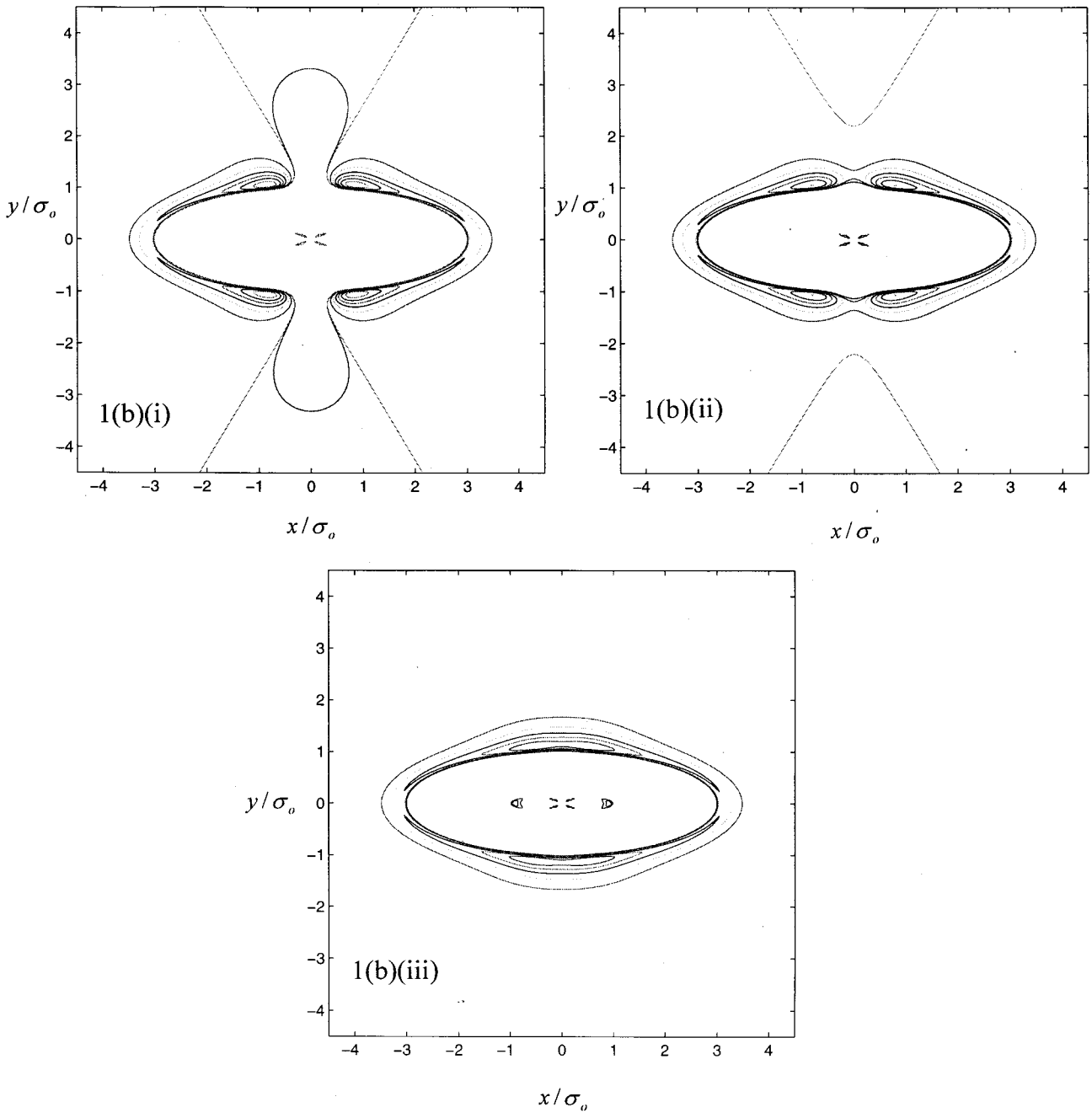

FIG. 1 (*Continued*).

where u_i^α is the α component of the unit vector along the symmetry axis of the molecule i. Q_{20}^2 was defined as the ensemble average of the largest eigenvalue of the **Q** tensor [30] and the director as the corresponding eigenvector $\hat{\mathbf{e}}$. Taking this as the laboratory Z direction the biaxial ordering was calculated following the method outlined in Ref. [31] from

$$Q_{22}^2 = \left\langle \frac{1}{2}(1+\cos^2\theta)\cos 2\phi \cos 2\psi - \cos\theta \sin 2\phi \sin 2\psi \right\rangle, \tag{5}$$

where θ, ϕ and ψ are the Euler angles of a typical molecule with respect to the laboratory axes.

Additionally the radial distribution function $g(r^*)$ and the longitudinal and transverse pair distribution functions $g_\parallel(r_\parallel^*)$ and $g_\perp(r_\perp^*)$ were calculated:

$$g(r^*) = \frac{V}{N^2}\left\langle \sum_i \sum_{j\neq i} \delta(\mathbf{r}-\mathbf{r}_{ij}) \right\rangle, \tag{6}$$

$$g_\parallel(r_\parallel^*) = \frac{V}{N^2}\left\langle \sum_i \sum_{j\neq i} \delta\left|[(\mathbf{r}-\mathbf{r}_{ij})\cdot\hat{\mathbf{e}}]\right| \right\rangle. \tag{7}$$

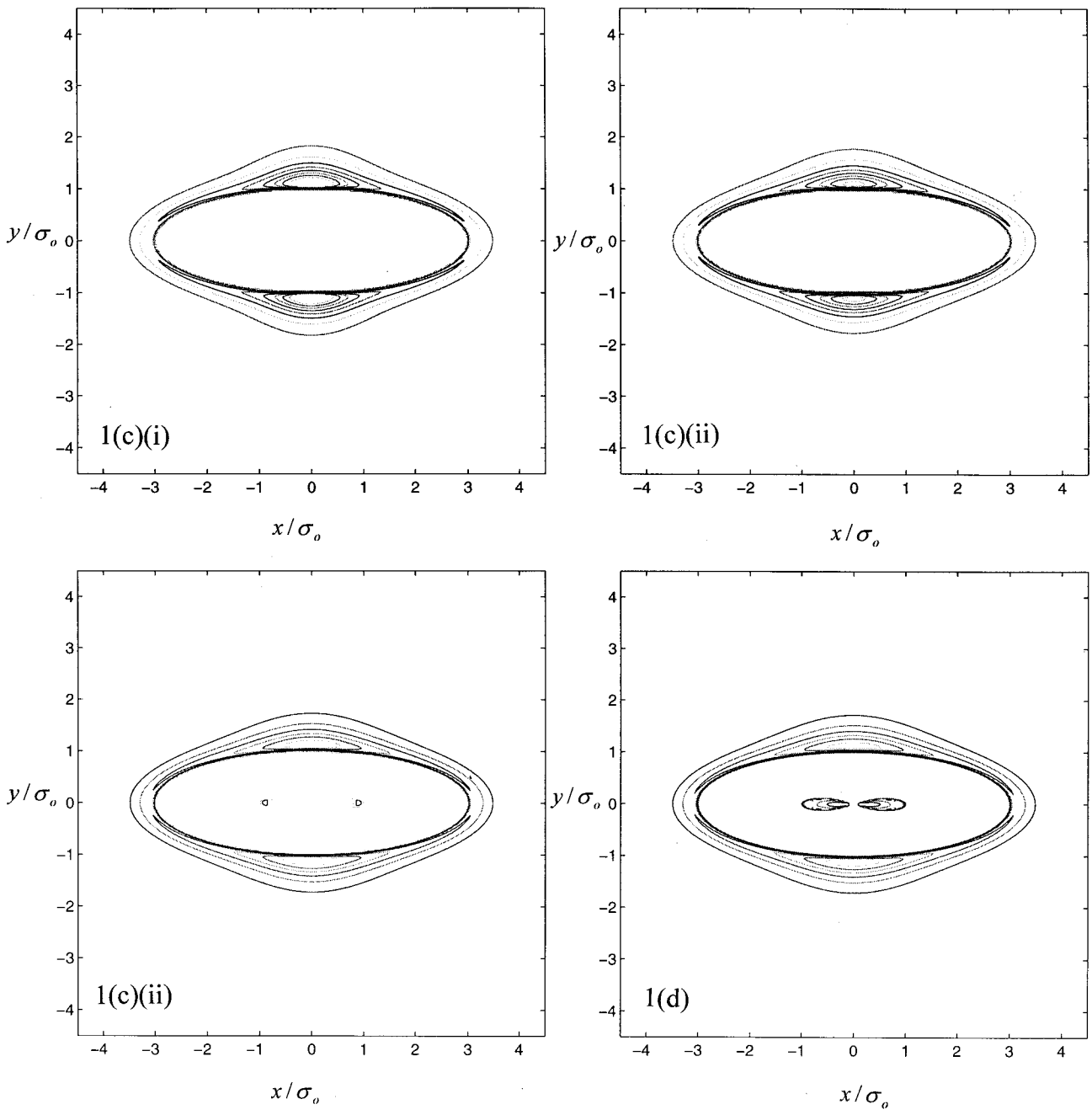

FIG. 1 (*Continued*).

A spherical cutoff was used for $g(r^*)$ while a cylindrical volume was used for $g_{\parallel}(r_{\parallel}^*)$ and $g_{\perp}(r_{\perp}^*)$ with the axis of the cylinder along the system director $\hat{\mathbf{e}}$, and $r_{\parallel}^*$ and $r_{\perp}^* \leqslant r_{\max}$. This enables the correlation between particles in adjacent layers to be considered in $g_{\parallel}(r_{\parallel}^*)$ and $g_{\perp}(r_{\perp}^*)$ and removes the weighting towards particles in the same layer.

IV. RESULTS AND DISCUSSION

Here the results are presented in two parts. In the first part the results for the quadrupolar fluid with $Q^* = -1.0$ are presented followed in the second part by those for the fluids with $Q^* = -0.5$ and -0.1.

A. Quadrupolar Gay-Berne rods with $Q^* = -1.0$

The variation in order parameters Q_{20}^2 and Q_{22}^2 as the system was cooled in shown in Fig. 2(a) and the corresponding variation in density is shown in Fig. 2(b). In order to provide a comparison with a Gay-Berne reference system with zero quadrupole, variations of the order parameter Q_{20}^2 and of density for this reference fluid are shown in the same figures. Brown *et al.*, [27] identified an isotropic phase, a narrow

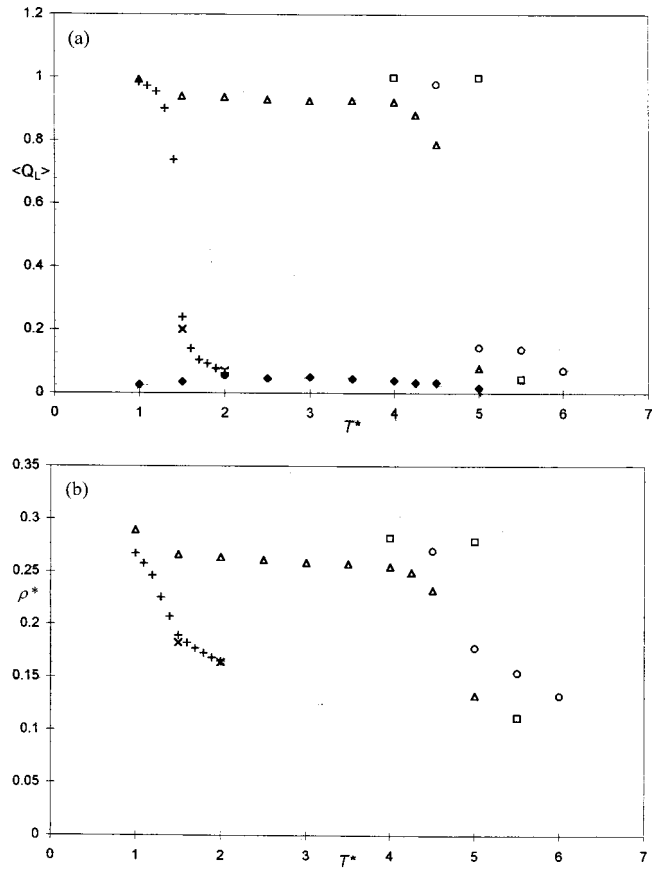

FIG. 2. The dependence of (a) orientational order parameters, and (b) density as a function of scaled temperature T^* for quadrupolar Gay-Berne rods with $|Q^*|$ of 1.0($\triangle Q_{20}^2$; $\blacklozenge Q_{22}^2$),$|Q^*|$ of 0.5($Q_{20}^2\bigcirc$) and $|Q^*|$ of 0.1($Q_{20}^2\square$) and for the nonpolar reference system (+). Two results labeled by $\times$ are additional results referred to in the text.

nematic region, and a smectic-*A* and a smectic-*B* region for a Gay-Berne fluid with an elongation of $\sigma_e/\sigma_s=4.0$. Two state points taken from their study (Table I) were found to agree closely with the results of the simulation of the reference fluid reported here. The state point at $T^*=1.5$ was just above the isotropic-nematic transition.

The phases of the reference fluid for a fixed pressure of $P^*=2.0$ can be distinguished by examining the order parameters and distribution functions. The Gay-Berne reference fluid exhibits an ordered phase at T^* of 1.4 ± 0.1 when the order parameter Q_{20}^2 increases to 0.738. The phase was identified as nematic from the distribution functions in Fig. 3(a)–(c). The orientationally averaged pair distribution function $g(r^*)$ in Fig. 3(a) shows liquidlike behavior and there is no structure apparent in $g_\perp(r_\perp^*)$ and $g_\parallel(r_\parallel^*)$. A smectic-*A* phase has been established at a temperature of $T^*=1.3$ since oscil-

TABLE I. State points for reference Gay-Berne fluid. The results labeled Δ were obtained from Ref. [27] by Monte Carlo techniques.

Pressure, P^*	Density, ρ^*	Order Parameter, Q_{20}^2	Temperature, T^*
2.0 Δ	0.1828(1)	0.201(2)	1.5
2.0	0.1894(20)	0.24(4)	1.5
2.0 Δ	0.1638(1)	0.070(2)	2.0
2.0	0.1649(20)	0.06(2)	2.0

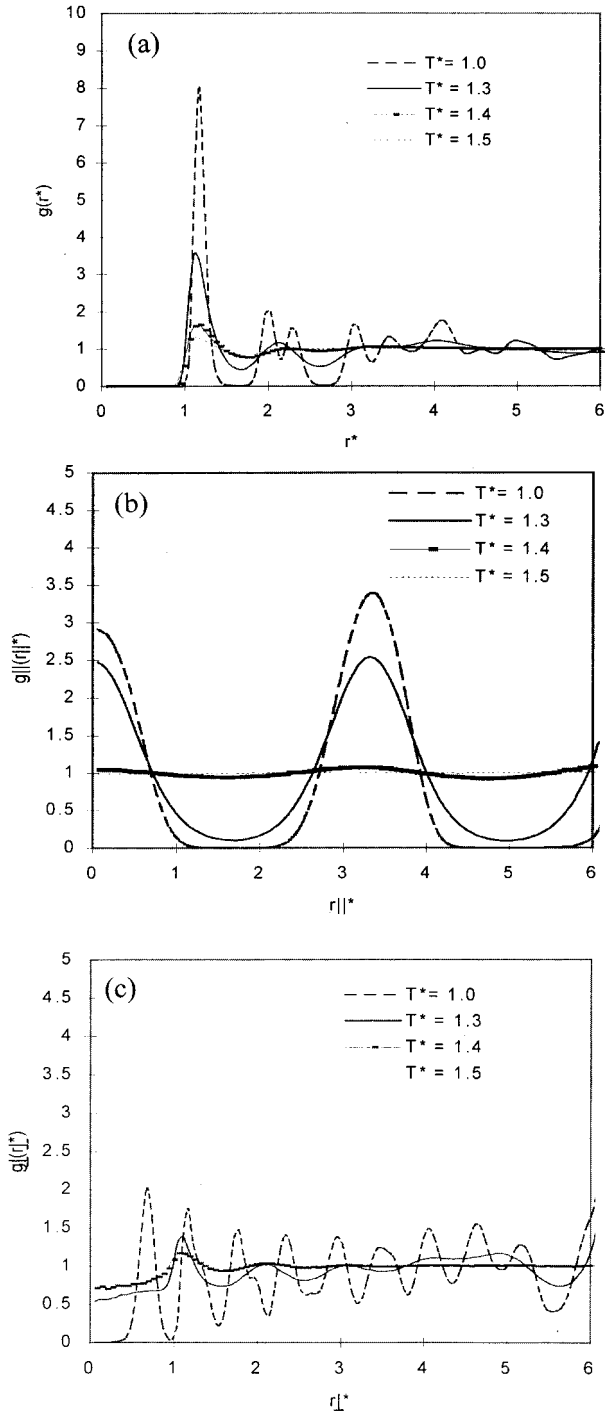

FIG. 3. (a) Pair distribution functions, (b) longitudinal pair distribution functions $g_\parallel(r_\parallel^*)$, and (c) transverse pair distribution functions $g_\perp(r_\perp^*)$ for the Gay-Berne reference system with zero quadrupole at a number of different temperatures (labeled on the plots).

lations can be seen in the longitudinal pair distribution function $g_{\parallel}(r_{\parallel}^*)$ in Fig. 3(b) but the behavior of $g_{\perp}(r_{\perp}^*)$ in Fig. 3(c) remains liquidlike. A third transition to a smectic-*B* phase is seen at temperatures less than 1.2 as indicated by the onset of additional transverse ordering shown in Fig. 3(c) for $T^*=1.0$. At the same time, structural features became apparent in the pair distribution function $g(r^*)$ [Fig. 3(a)] with a split in the second peak at $r^*\approx 2.0$ and 2.3 characteristic of the second- and third-shell neighbors in a smectic-*B* phase. Crystal and hexatic variants of the smectic-*B* phase are distinguished by long-range and quasi-long-range positional order but the size of the simulation is such that no distinction can be made between the two.

The quadrupolar system exhibits an isotropic phase at $T^*=5.0\pm 0.5$ but undergoes a weak first-order transition into an ordered phase at $T^*=4.5\pm 0.5$. This is indicated by a discontinuity in the density and an increase in the order parameter Q_{20}^2 to 0.786. It is apparent that the presence of the quadrupole has a marked effect on the temperature of the transition to an ordered phase, raising it considerably. The phase is identified as nematic since no oscillations are established in $g_{\parallel}(r_{\parallel}^*)$ and $g_{\perp}(r_{\perp}^*)$ remains liquidlike as shown in Fig. 4(b) and 4(c), respectively. The transition occurs at a higher density of 0.2325 (1) in the quadrupolar fluid compared to 0.2074 (1) for the reference fluid. This agrees with the trend [19] shown in the simulation of a soft spherical dipolar fluid on the addition of a quadrupole. The side-to-side configuration for quadrupoles effectively occupies a higher volume because of the central maximum and may account for this trend. As the temperature is lowered, a smectic-*A* phase is clearly established in the temperature range from 4.0 to 1.5. Pronounced oscillations are seen in the longitudinal distribution function $g_{\parallel}(r_{\parallel}^*)$ shown in Fig. 4(b). The amplitude of the oscillations remains constant over this temperature range. The transverse pair distribution function $g_{\perp}(r_{\perp}^*)$ also remains liquidlike over this extended region [Fig. 4(b)]. Thus the region is identified as an extended smectic-*A* phase.

When the temperature is lowered to 1.0 the onset of order in the transverse pair distribution function occurs, as shown in Fig. 4(c). At the same time structural features became apparent in the pair distribution function $g(r^*)$ [Fig. 4(a)]. In this case the second- and higher co-ordination shells are indicated by a second peak at $r^*\approx 1.6$ and a split third peak at $r^*\approx 2.2-2.3$. This pattern is characteristic of cubic rather than hexagonal packing. Figure 5(a) illustrates a plan view of the vectors $\hat{\mathbf{v}}_i$ acting through the centers-of-mass of the molecules and perpendicular to the molecular axes of symmetry $\hat{\mathbf{u}}_i$. It is apparent that the quadrupolar fluid has a final cubic structure in comparison to the more usual hexagonal structure. The structure of cubic packing allows the transverse quadrupoles to form in-plane '*T*' configurations, with favored negative interaction energy. The proposed structure is illustrated in a plan view in Fig. 5(b) looking down the major axis of the particles. It comprises two subcells of lattices with alternating quadrupoles in '*T*' configurations. Overall the structure then has net zero biaxiality in a given plane and

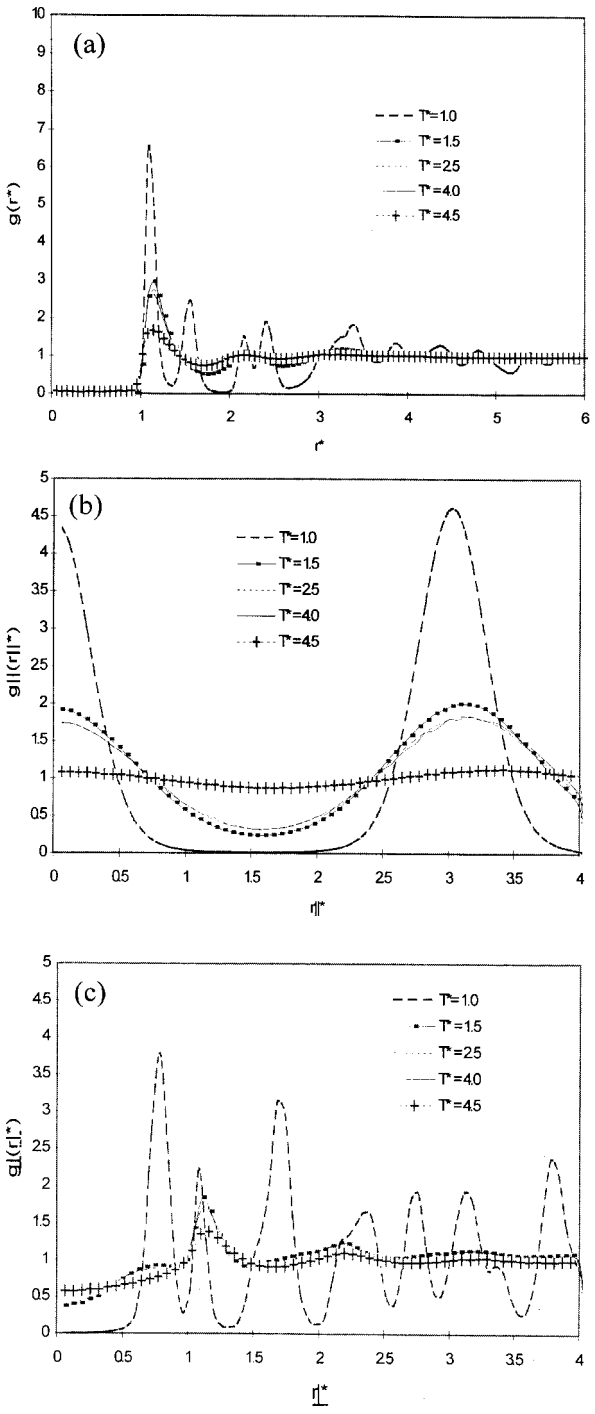

FIG. 4. (a) Pair distribution functions, (b) longitudinal pair distribution functions $g_{\parallel}(r_{\parallel}^*)$, and (c) transverse pair distribution functions $g_{\perp}(r_{\perp}^*)$ for the quadrupolar Gay-Berne system with quadrupole $Q^*=-1.0$ at a number of different temperatures (labeled on the plots).

no significant overall biaxiality was observed for any of the phases of the quadrupolar fluid.

At present few compounds [32,33] are known to exhibit a cubic lattice and little is known about the detailed molecular arrangement. They should probably be labeled '*D*' rather than smectic-'*D*' if the phase has overall cubic symmetry. Some compounds [32] have a strong, lateral ring-NO_2 or CN

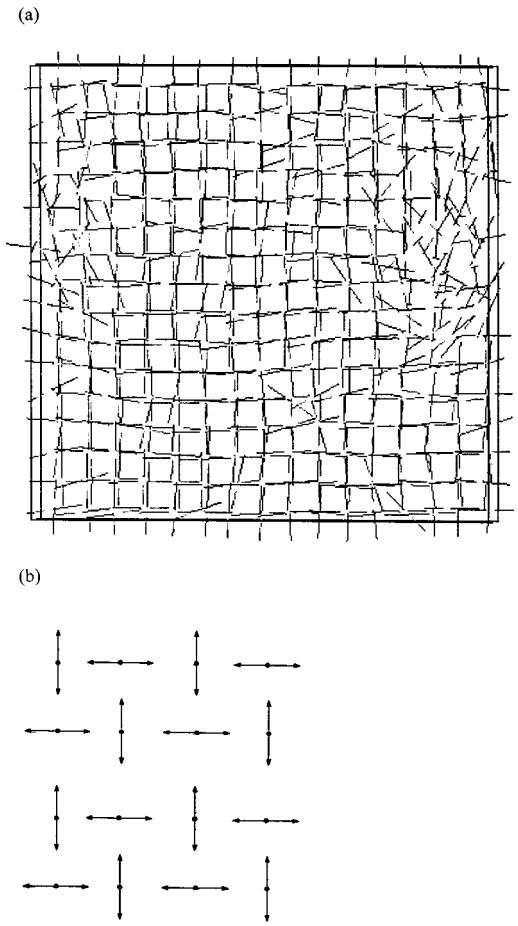

FIG. 5. (a) A typical configuration of a plan view of the vectors $\hat{\mathbf{v}}_i$ acting through the centers-of-mass of the molecules and perpendicular to the molecular axes of symmetry $\hat{\mathbf{u}}_i$ for the quadrupolar Gay-Berne system with quadrupole $Q^*=-1.0$ at $T^*=1.0$; (b) A plan view down the major molecular axes of a proposed structure for the arrangement of quadrupoles within a plane.

dipole and associated quadrupole that may be critical in determining the structure.

The simulation results indicate that a large transverse quadrupole has a dramatic effect on the stability of the smectic-*A* phase formed by the Gay-Berne fluid and stabilizes a final cubic lattice allowing the formation of '*T*' arrangements of quadrupoles in-plane. In contrast the side-to-side configuration shows a marked change in shape of the zero contour. Figures 1(b)(i) illustrates the replacement of the central minimum with a central maximum and two adjacent minima, and hence the side-to-side arrangement of quadrupoles is strongly disfavored as an in-plane configuration.

B. Quadrupolar Gay-Berne rods with $Q^*=-0.5$ and -0.1

The variation in order parameter Q_{20}^2 as the weakly quadrupolar fluid systems were cooled is shown in Fig. 2(a) and the corresponding variation in density is shown in Fig. 2(b). They both exhibit an isotropic phase at $T^*=5.5\pm0.5$ but undergo a first-order transition into an ordered phase at $T^*=4.5\pm0.5$ and $T^*=5.0\pm0.5$, for $|Q^*|$ of 0.5 and 0.1, respectively. This is indicated by a discontinuity in the density

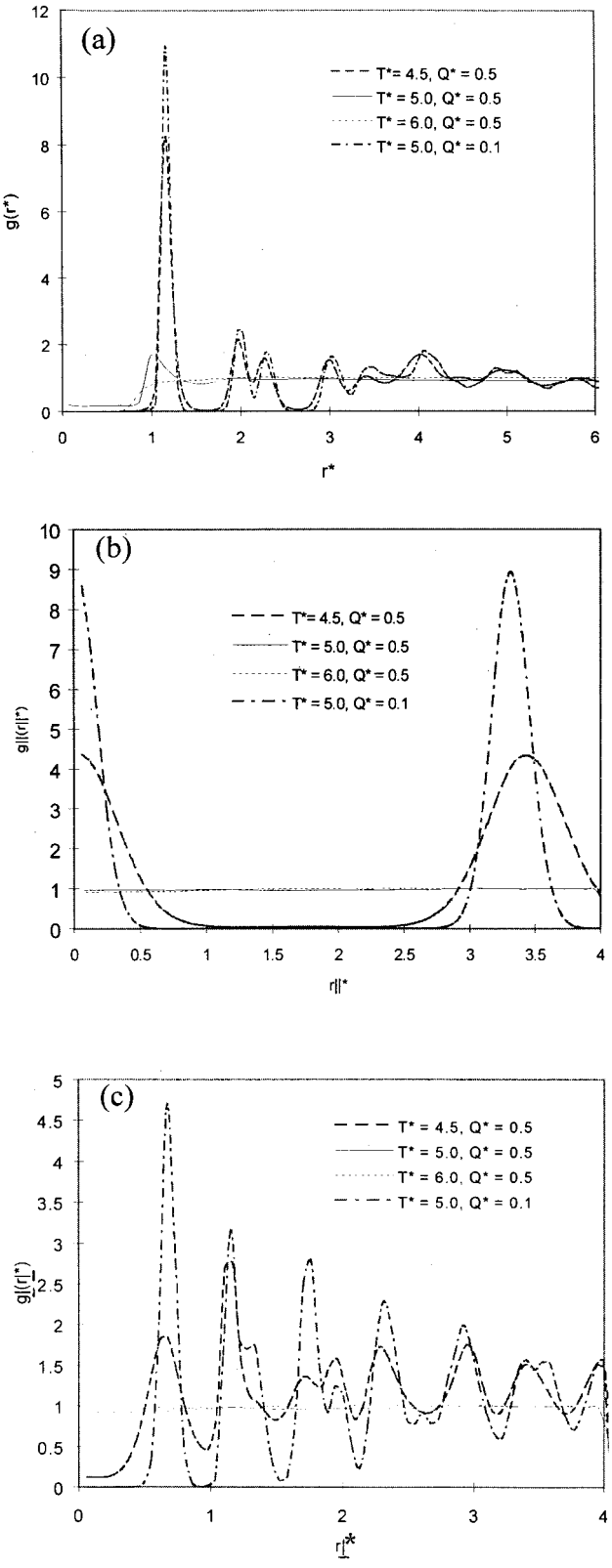

FIG. 6. (a) Pair distribution functions, (b) longitudinal pair distribution functions $g_{\parallel}(r_{\parallel}^*)$, and (c) transverse pair distribution functions $g_{\perp}(r_{\perp}^*)$ for the quadrupolar Gay-Berne system with quadrupole $Q^*=-0.1$ and -0.5, at a number of different temperatures (labeled on the plots).

and an increase in the order parameter Q_{20}^2 to 0.976 ± 0.01 and 0.997 ± 0.001, respectively. It is apparent that the presence of the weaker quadrupoles still considerably raises the temperature of the transition to an ordered phase. A new generic Corner potential [34], which generates a shape analogous to a uniaxial shape generated from Figs. 1(b)(i) or (ii) by rotation about the major axis also leads to a considerable rise in temperature of the onset of ordered mesophases. The disfavored side-to-side quadrupole configuration in combination with the favored '*T*' quadrupole configuration may be influencing this transition. The side-to-side configuration effectively occupies a higher volume at any given temperature because of the central maximum, thus tending to a higher temperature of onset of order. It is interesting to note that all thermotropic liquid crystals contain aromatic groups with transverse quadrupoles, and that polar groups are present in lyotropic liquid crystals such as the tobacco mosaic virus.

Both systems undergo a transition into a highly ordered system with hexagonal packing. This is apparent from the structural features in the pair distribution function $g(r^*)$ [Fig. 6(a)]. A split is seen in the second peak at $r^* \approx 2.0$ and 2.3, characteristic of the second- and third-shell neighbors in a smectic-*B* phase and similar to the lattice occupied by the reference nonpolar fluid. It is apparent from Figs. 6(b) and 6(c) that no nematic or smectic-*A* phase is present, unlike the reference Gay-Berne fluid or the strongly quadrupolar Gay-Berne fluid.

V. CONCLUSIONS

We have performed a study of the effect of the magnitude of a transverse quadrupole upon the mesophase formation of a quadrupolar Gay-Berne fluid. We have studied the effect of a range of quadrupole magnitudes similar to that seen in groups commonly found in liquid crystal molecules. We have found that the presence of a quadrupole increases the temperature of onset of the nematic and smectic phases. A large magnitude quadrupole stabilizes the smectic-*A* phase and influences the final crystal structure forming a cubic rather than the more usual hexagonal structure. The quadrupolar fluid effectively occupies a larger volume than the equivalent reference fluid since the side-to-side quadrupolar configuration is strongly disfavored.

ACKNOWLEDGMENTS

We are grateful for the support of the U.K. Engineering and Physical Sciences Research Council award, GR/L76693 and for the support of the Defense Evaluation research Agency, Malvern, U.K. We are also grateful for useful conversations with J. W. G. Goodby and M. Grayson

APPENDIX

The strength anisotropy function,

$$\varepsilon(\hat{\mathbf{u}}_i, \hat{\mathbf{u}}_j, \hat{\mathbf{r}}_{ij}) = \varepsilon_0 \varepsilon_1^{\nu}(\hat{\mathbf{u}}_i, \hat{\mathbf{u}}_j) \varepsilon_2^{\mu}(\hat{\mathbf{u}}_i, \hat{\mathbf{u}}_j, \hat{\mathbf{r}}_{ij}) \tag{A1}$$

Here the powers μ and ν are adjustable exponents and ε_0 is a constant.

The first component of ε,

$$\varepsilon_1(\hat{\mathbf{u}}_i, \hat{\mathbf{u}}_j) = [1 - \chi^2 (\hat{\mathbf{u}}_i \cdot \hat{\mathbf{u}}_j)^2]^{-1/2} \tag{A2}$$

and the second,

$$\varepsilon_2(\hat{\mathbf{u}}_i, \hat{\mathbf{u}}_j, \hat{\mathbf{r}}_{ij}) = \left[1 - \frac{\chi'}{2} \left\{ \frac{(\hat{\mathbf{r}}_{ij} \cdot \hat{\mathbf{u}}_i + \hat{\mathbf{r}}_{ij} \cdot \hat{\mathbf{u}}_j)^2}{1 + \chi' \hat{\mathbf{u}}_i \cdot \hat{\mathbf{u}}_j} + \frac{(\hat{\mathbf{r}}_{ij} \cdot \hat{\mathbf{u}}_i - \hat{\mathbf{r}}_{ij} \cdot \hat{\mathbf{u}}_j)^2}{1 - \chi' \hat{\mathbf{u}}_i \cdot \hat{\mathbf{u}}_j} \right\} \right]. \tag{A3}$$

The parameter χ', is given by

$$\chi' = [1 - (\varepsilon_e / \varepsilon_s)^{1/\mu}] / [1 + (\varepsilon_e / \varepsilon_s)^{1/\mu}] \tag{A4}$$

and reflects the anisotropy in the attractive forces where $\varepsilon_e / \varepsilon_s$ is the ratio of the end-to-end and side-to-side well depths.

The orientation dependent range parameter,

$$\sigma(\hat{\mathbf{u}}_i, \hat{\mathbf{u}}_j, \hat{\mathbf{r}}_{ij}) = \sigma_0 \left[1 - \frac{\chi}{2} \left\{ \frac{(\hat{\mathbf{r}}_{ij} \cdot \hat{\mathbf{u}}_i + \hat{\mathbf{r}}_{ij} \cdot \hat{\mathbf{u}}_j)^2}{1 + \chi \hat{\mathbf{u}}_i \cdot \hat{\mathbf{u}}_j} + \frac{(\hat{\mathbf{r}}_{ij} \cdot \hat{\mathbf{u}}_i - \hat{\mathbf{r}}_{ij} \cdot \hat{\mathbf{u}}_j)^2}{1 - \chi \hat{\mathbf{u}}_i \cdot \hat{\mathbf{u}}_j} \right\} \right]^{-1/2}. \tag{A5}$$

Here χ is given by

$$\chi = [(\sigma_e / \sigma_s)^2 - 1] / [(\sigma_e / \sigma_s)^2 + 1] \tag{A6}$$

and reflects the shape anisotropy, where σ_e / σ_s is the ratio of separations when $U_{\mathrm{GB}} = 0$ for the molecules in the end-to-end and side-to-side configurations. For prolate ellipsoids considered here $\sigma_0 = \sigma_s$.

[1] J. W. Goodby, *Ferroelectric Liquid Crystals* edited by Goodby *et al.* (Gordon and Breach, Philadelphia, 1991).
[2] W. L. McMillan, Phys. Rev. A **8**, 1921 (1973).
[3] D. Cabib and L. Bengiugiu, J. Phys. (France) **38**, 419 (1977).
[4] B. W. Van Der Meer and G. Vertogen, J. Phys. (Paris), Colloq. **40**, 222 (1979).
[5] A. Poniewierski and T. J. Sluckin, Mol. Phys. **73**, 199 (1991).
[6] G. Barbero and G. Durand, Mol. Cryst. Liq. Cryst. **179**, 57 (1990).
[7] A. Wulf, Phys. Rev. A **11**, 36 (1975).
[8] A. M. Somoza and P. Tarazona, Phys. Rev. Lett. **61**, 2566 (1988).
[9] D. J. Photinos and E. T. Samulski, Science **270**, 782 (1995).
[10] A. Gil-Villegas, S. C. McGrother, and G. Jackson, Mol. Phys. **92**, 723 (1997).
[11] S. C. McGrother and G. Jackson, Phys. Rev. Lett. **76**, 4183 (1996).
[12] J. J. Weis, D. Levesque, and G. J. Zarragoicoechea, Phys. Rev.

Lett. **69**, 913 (1992).
[13] R. Beradi, R. Orlandi, and C. Zannoni, Chem. Phys. Lett. **261**, 357 (1996).
[14] K. Satoh, M. Shigeru, and S. Kondo, Liq. Cryst. **20**, 767 (1996); K. Satoh, S. Mita, and S. Kondo, Chem. Phys. Lett. **225**, 99 (1996).
[15] S. Gupta, W. B. Sediawan, and E. Mclaughlin, Mol. Phys. **65**, 961 (1998).
[16] J. H. Williams, J. K. Cockcroft, and A. N. Fitch, Angew. Chem. **31**, 1655 (1992).
[17] M. A. Bates and G. R. Luckhurst, Liq. Cryst. **24**, 22 (1998).
[18] C. Vega, B. Garzon, S. Largo, and P. A. Monza, J. Mol. Liq. **76**, 157 (1998).
[19] D. Wei, Mol. Cryst. Liq. Cryst. **269**, 89 (1995).
[20] M. P. Neal and A. J. Parker, Chem. Phys. Lett. **294**, 277 (1998).
[21] G. R. Luckhurst, 1998 (private communication).
[22] J. G. Gay and B. J. Berne, J. Chem. Phys. **74**, 3316 (1981).
[23] A. D. Buckingham, Adv. Chem. Phys. **12**, 107 (1978).
[24] S. L. Price, A. J. Stone, and A. Alderton, Mol. Phys. **52**, 987 (1984).
[25] R. Hashim, G. R. Luckhurst, and S. J. Romano, Chem. Soc. Faraday Trans, **91**, 2141 (1995).
[26] E. De Miguel, L. F. Rull, M. K. Chalam, and K. E. Gubbins, Mol. Phys. **74**, 405 (1991).
[27] J. T. Brown, M. P. Allen, E. M. del Rio, and E. D. Miguel, Phys. Rev. E **57**, 6685 (1998).
[28] G. R. Luckhurst and P. S. J. Simmonds, Mol. Phys. **80**, 233 (1993).
[29] A. Chablo, D. W. J. Cruickshank, A. Hinchcliffe, and R. W. Munro, Chem. Phys. Lett. **78**, 424 (1981).
[30] C. Zannoni, *The Molecular Physics of Liquid Crystals*, edited by G. R. Luckhurst and G. W. Gray (Academic Press, New York, 1979) Chap. 3.
[31] M. P. Allen, Liq. Cryst. **8**, 499 (1990).
[32] S. Chandrasekhar, *Liquid Crystals* (Cambridge University Press, Cambridge, 1992).
[33] B. Donnio and D. W. Bruce, J. Mater. Chem. **8(9)**, 1993 (1998).
[34] A. H. Ghahrai, G. R. Luckhurst, and G. Saielli, British Liquid Crystal Society, 15th Annual Conference, University of Strathclyde, Poster 3, 2000.